Effects of periodic perturbations on the oscillatory behavior in the $NO+H_2$ reaction on Pt(100)

M. C. Lemos,* A. Córdoba, and J. A. de la Torre
Departamento de Física de la Materia Condensada, Universidad de Sevilla, P.O. Box 1065, 41080 Sevilla, Spain
(Received 22 June 2009; published 25 March 2010)

The mean field model proposed by Makeev and Nieuwenhuys [J. Chem. Phys. **108**, 3740 (1998)] simulates the oscillatory behavior experimentally observed in the $NO+H_2$ reaction on the surface Pt(100). This model reproduces quite well the kinetic oscillations and the transition to chaos via the Feigenbaum route, that is to say, through bifurcations involving period doubling. From this model, we analyze the response of the natural oscillations of period-1 (P1, one maximum) to periodic perturbations superposed to the partial pressure of one of the reactants. The perturbed model reproduces the periodic states found in the autonomous model, the route to chaos through bifurcations with period doubling, and the appearance of chaos via the route of intermittency, which shows alternation of periodic oscillations with intervals of disordered oscillations in the same time evolution. Experimentally it has been observed that the reaction shows a great sensitivity to reactant partial pressures and temperature. In experimental conditions slightly different to those considered in Makeev and Nieuwenhuys (MN) model, oscillations with period-3 (P3, three maxima) have been observed. At $T=457$ K and certain pressures, these P3 oscillations do not appear in MN model, although they appear at $T=456$ K. The same effect (P3 oscillations) is obtained at $T=457$ K in our perturbed model, due to the modulation of p_{H_2}. In a second step we show how the modulation of the perturbing frequency influences on the oscillations P1 of the perturbed system. The results show that the periodic behavior loses its regularity at low values of the normalized amplitude and of the modulated frequency of the perturbation. Other aspect observed in the perturbed model is that the amount of products varies in relation to nonperturbed model. When the oscillations are periodic or they follow the Feigenbaum route to chaos, the production average decreases or slightly increases, whereas it always increases if there are intermittencies, the most significant percentage increase being for NH_3 (nearly 10%).

DOI: 10.1103/PhysRevE.81.036116 PACS number(s): 82.20.Wt, 05.45.−a, 82.40.Bj

I. INTRODUCTION

Catalytic reduction of nitric oxide by hydrogen on surface Pt(100) has been studied experimentally and theoretically [1–8]. For certain experimental conditions a complex dynamic behavior has been observed. This dynamics includes, among others, regular oscillations, chaotic behavior and formation of spatial patterns.

Kinetic oscillations have been observed at pressures of the reactant gases in the range 10^{-6} to 10^{-5} mbar and at temperature ranging from 430 to 500 K. Previous theoretical studies [9,10] suggested that the kinetic oscillations are due to the surface phase transition (SPT) $(1\times1)\Leftrightarrow$hex. However Cobden *et al.* [4] proposed an alternate view. They used a "vacancy model" where oscillations are due to the self-catalytic surface reaction that increases the number of vacant sites which are required for NO dissociation on the (1×1) phase, although they did not propose any mathematical model of that mechanism. Later Makeev and Nieuwenhuys (MN) developed a mathematical model (six variables model) [11] in order to demonstrate that the self-catalytic decomposition of NO through vacant sites was one of the most important conditions to cause the system oscillations and necessary to kept them. The other major property was that the activation energies for desorption and dissociation of NO depend on the surface coverage.

Catalytic reduction of NO by CO on Pt(100) exhibits a dynamic behavior similar to that observed in the reaction $NO+H_2/Pt(100)$. For the system NO+CO Fink *et al.* [12] demonstrated that the oscillatory behavior appears in two windows. In the window at low temperature (about 400 K) the system shows an oscillatory behavior without the SPT is observed and in the window at high temperature (about 450 K) the SPT is detected during the kinetic oscillations. Similarly, in the system $NO+H_2/Pt(100)$ oscillations take place on the (1×1) surface when temperature is relatively low ($T<480$ K). In fact, MN [11] demonstrated that the $(1\times1)\Leftrightarrow$hex SPT is not essential to produce oscillatory behavior in the window at low temperature and, therefore, they did not included the SPT in their model. This was formulated in terms of six differential equations for the time evolution of the surface adsorbates in the (1×1) phase. This model can reproduce quite well several experimental observations concerning the $NO+H_2$ reaction. These observations include, among others, temperature programmed desorption (TPD) and temperature programmed reaction (TPR) spectra, the temperature dependence of the oscillatory period, and a transition from period-1 oscillations to chaos through period doubling bifurcations when the H_2 pressure is decreased.

Nevertheless, the model does not reproduce the experimental hysteresis in the H_2O production rate and the surface structure since it does not assume the SPT. Obviously, the hysteresis is associated with the changes in the surface structure during a heat-cool cycle. In order to model the hysteresis, MN extended their model to include the adsorbate-induced $(1\times1)\Leftrightarrow$hex SPT in a subsequent paper (eight variables model) [13]. They demonstrated that at temperatures higher than 480 K (when the adsorbate coverages become low), oscillations take place on a largely hex-reconstructed surface. Decreasing the temperature induces an

*lemos@us.es

increase in the adsorbate coverage and, as a result, an increase in the fraction of the (1×1) phase. At relatively low temperatures ($420\ \mathrm{K}<T<480\ \mathrm{K}$), oscillations take place on a surface that is completely in the (1×1) surface. The results of the eight variables model show that the effect of surface restructuring is not essential for producing oscillatory behavior in the low temperature window, although oscillations are observed on a largely hex-reconstructed surface at the upper part of the range of temperatures. So, according to MN [13], the main oscillation mechanism is determined by the reactions occurring within the nonideal adlayer on the (1×1) surface of Pt(100), where the autocatalytic formation of vacant sites which are required for NO dissociation plays a decisive role.

The periodic perturbation of the reaction kinetics through the variation in some external control parameter, as, for example, the pressure of a reactant or the gas temperature, is one of the tools more frequently used in the study of heterogeneous catalytic reactions [14]. The results obtained in this field refer generally to perturbations of oscillations with period-1 (P1) through the periodic modulation of one of the control parameters. In experiments focused on the study of the complex behavior in oscillatory catalytic reactions, the technique of the periodic forcing is used as for stabilizing oscillations P1, which is achieved if both external and internal frequencies coincide, as for generating quasiperiodic oscillations or to control chaos. In this case, one intends to stabilize the unstable periodic orbits contained in the chaotic attractors of the system.

Too one of the goals of applying periodic perturbations on a reaction is to see whether these perturbations can be used to improve the performance of this reaction, e.g., increasing the amount of resultant products [14].

The effect of periodic perturbations on the oscillatory kinetics of the $NO+H_2$ reaction on Pt(100) was analyzed by Zhdanov [15] through Monte Carlo simulations. In his simulations, Zhdanov used a model by taking into account the surface reconstruction [$(1\times1)\Leftrightarrow$hex SPT]. These Monte Carlo simulations only illustrated the effect of perturbations on period-2 oscillations. With this purpose, Zhdanov applied a periodic modulation in the partial pressure of the NO gas. The simulations were carried out with five frequencies and three modulation amplitudes. The results of simulations showed that period-2 oscillations are sustained if the external frequency equals the main internal frequency. In contrast, perturbations with other frequencies may easily change the period-2 oscillations. In particular, period-2 oscillations may be converted to period-1 oscillations or period-3 oscillations. Finally, quasiperiodic or chaotic behaviors are not observed.

Transitions to chaos in dissipative systems can take place according to three scenarios. One of them is the Feigenbaum route [16] where chaos is reached through bifurcations involving period doubling. Other approximation to chaos is the called intermittency route [17], in which periodic behavior alternates with disordered bursts more or less short. The number of these irregular bursts can be increased through the change of some external control parameter up to the signal becomes completely chaotic. A third scenario is the Ruelle-Takens-Newhouse route [18,19], in which the appearance of quasiperiodic behavior precedes the emergence of an strange attractor.

The aim of our study is analyzing the influence of the periodic forcing technique, which we have previously applied to the reactions $CO+O_2$ [20,21] and N_2O+H_2 [22], has on the oscillatory behavior found in the reaction $NO+H_2$, starting from the first mean field model proposed by MN [11].

This paper is divided as follow. First, we use the MN model to reproduce the periodic and chaotic oscillations which are observed in the $NO+H_2/Pt(100)$ system without considering the $(1\times1)\Leftrightarrow$hex SPT. The characteristics and the results of the nonperturbed model are explained in Sec. II. In Sec. III we show the results obtained when the natural oscillations P1 are periodically perturbed. Later, the perturbing frequency is modulated and the way as this perturbation affects to the oscillations P1 observed in the perturbed system is analyzed. Finally, in Sec. IV we summarize some conclusions.

II. MODEL OF MAKEEV AND NIEUWENHUYS ON THE $NO+H_2/Pt(100)$-(1×1) REACTION

Makeev and Nieuwenhuys modeled the reaction according to the following set of elemental steps:

$$\mathrm{NO(g)} + V \rightarrow \mathrm{NO(ads)}, \tag{1}$$

$$\mathrm{H_2(g)} + 2V \rightarrow \mathrm{H(ads)} + \mathrm{H(ads)}, \tag{2}$$

$$\mathrm{NO(ads)} \rightarrow \mathrm{NO(g)} + V, \tag{3}$$

$$\mathrm{H(ads)} + \mathrm{H(ads)} \rightarrow \mathrm{H_2(g)} + 2V, \tag{4}$$

$$\mathrm{N(ads)} + \mathrm{N(ads)} \rightarrow \mathrm{N_2(g)} + 2V, \tag{5}$$

$$\mathrm{NO(ads)} + V \rightarrow \mathrm{N(ads)} + \mathrm{O(ads)}, \tag{6}$$

$$\mathrm{N(ads)} + \mathrm{O(ads)} \rightarrow \mathrm{NO(ads)} + V, \tag{7}$$

$$\mathrm{O(ads)} + \mathrm{H(ads)} \rightarrow \mathrm{OH(ads)} + V, \tag{8}$$

$$\mathrm{N(ads)} + \mathrm{H(ads)} \rightarrow \mathrm{NH(ads)} + V, \tag{9}$$

$$\mathrm{NH(ads)} + V \rightarrow \mathrm{N(ads)} + \mathrm{H(ads)}, \tag{10}$$

$$\mathrm{NH(ads)} + \mathrm{H(ads)} \rightarrow \mathrm{NH_2(ads)} + V, \tag{11}$$

$$\mathrm{NH_3(ads)} \rightarrow \mathrm{NH_3(g)} + V, \tag{12}$$

$$\mathrm{NH_2(ads)} + \mathrm{H(ads)} \rightarrow \mathrm{NH_3(ads)} + V, \tag{13}$$

$$\mathrm{OH(ads)} + \mathrm{H(ads)} \rightarrow \mathrm{H_2O(ads)} + V, \tag{14}$$

$$\mathrm{H_2O(ads)} \rightarrow \mathrm{H_2O(g)} + V, \tag{15}$$

where V is a vacant site on the Pt(100)-(1×1) surface, (ads) denotes an adsorbed particle on the surface and (g) indicates the gas phase. NO(g) and H_2(g) are the reactants in the gas

phase with partial pressures p_{NO} and p_{H_2}, respectively. The reaction products are $N_2(g)$, $NH_3(g)$ and $H_2O(g)$.

The mechanism of the reaction includes the adsorption/desorption processes of NO and H_2, dinitrogen formation through combination of two adjacent adatoms of nitrogen, reversible dissociation of NO(ads) producing N and O adatoms, ammonia formation through reversible hydrogenation [via intermediates NH(ads) and NH_2(ads)], and water formation through hydrogenation of O(ads) [via intermediate OH(ads)].

In order to reduce the number of variables in the model, desorption of H_2O(ads) [Eq. (15)], and hydrogenation of both intermediates OH(ads) [Eq. (14)] and NH_2(ads) [Eq. (13)] are assumed quick processes and they are not taken into account for the whole reaction. Because of these assumptions, only six species are considered, NO(ads), H(ads), N(ads), O(ads), NH(ads), NH_3(ads), and their corresponding surface densities n_p, being $p=\mathrm{NO},\mathrm{H},\mathrm{N},\mathrm{O},\mathrm{NH},\mathrm{NH_3}$ or $p=1,\ldots,6$.

The appearance of oscillations in the model arises from the demand of two important conditions: the need of vacant sites for the self-catalytic dissociation of NO and the dependence of the activation energies on the coverage for the processes of dissociation and desorption of NO. These nonlinearities are explained in terms of lateral interactions in the adlayer. So, the model takes into account the nonlinearity of the adlayer through the parameters of lateral interaction $\varepsilon_{\alpha p}$ as we will see afterwards. If the step α proceeds in some site of the lattice, then one assumes that each next nearest neighbor of type p decreases its activation energy E_α in the value $\varepsilon_{\alpha p}$. At a microscopic scale, these energetic parameters show the effective influence of the neighborhood on the activation energies of the elemental steps of the reaction. The value $\varepsilon_{\alpha p}$ may be considered as the difference of the lateral interactions between both activated and fundamental states.

According to the reaction mechanism proposed, the time change in the surface densities along the reaction is described through six coupled differential equations:

$$\frac{dn_{NO}}{dt} = R_1 - R_3 - R_6 + R_7, \tag{16}$$

$$\frac{dn_H}{dt} = 2R_2 - 2R_4 - 2R_8 - R_9 + R_{10} - 2R_{11}, \tag{17}$$

$$\frac{dn_N}{dt} = R_6 - 2R_5 - R_7 - R_9 + R_{10}, \tag{18}$$

$$\frac{dn_O}{dt} = R_6 - R_7 - R_8, \tag{19}$$

$$\frac{dn_{NH}}{dt} = R_9 - R_{10} - R_{11}, \tag{20}$$

TABLE I. Kinetic parameters used in the model.

Reaction step, α	ν_α (s^{-1})	E_α (kcal/mol)
1	2.14×10^5 $mbar^{-1}$	0
2	8.28×10^5 $mbar^{-1}$	0
3	1.7×10^{15}	37
4	10^{12}	25
5	10^{13}	24
6	2×10^{15}	28
7	2×10^{15}	23
8	10^{13}	13
9	10^{9}	15
10	10^{13}	29
11	10^{9}	17.7
12	10^{9}	19

$S_{NO}k_1 = 1.93\times10^5$ $mbar^{-1}$ s^{-1}, $S_{H_2}k_2 = 1.656\times10^5$ $mbar^{-1}$ s^{-1}

$$\frac{dn_{NH_3}}{dt} = R_{11} - R_{12}. \tag{21}$$

The rates R_α of the elemental steps [Eqs. (1)–(12)] of the reaction are expressed as

$$R_1 = k_1 p_{NO} S_{NO} n_V, \quad R_2 = k_2 p_{H_2} S_{H_2} n_V^2,$$

$$R_3 = k_3 I_3 n_{NO}, \quad R_4 = k_4 I_4 n_H^2,$$

$$R_5 = k_5 I_5 n_N^2, \quad R_6 = k_6 I_6 n_{NO} n_V,$$

$$R_7 = k_7 n_N n_O, \quad R_8 = k_8 n_O n_H,$$

$$R_9 = k_9 n_N n_H, \quad R_{10} = k_{10} n_{NH} n_V,$$

$$R_{11} = k_{11} n_{NH} n_H, \quad R_{12} = k_{12} n_{NH_3},$$

where

$$n_V = 1 - n_{NO} - n_H - n_N - n_O - n_{NH} - n_{NH_3},$$

$$k_\alpha = \nu_\alpha \exp\left\{\frac{-E_\alpha}{RT}\right\}, \quad \forall\ \alpha = 1,\ldots,12,$$

$$I_\alpha = \left\{ n_V + \sum_{p=1}^{6} n_p \exp\left\{\frac{\varepsilon_{\alpha p}}{RT}\right\} \right\}^{m_\alpha}.$$

Here, m_α is the number of next nearest sites. The quantities I_α determine the influence of the lateral interactions on the rates of the elemental processes. The gas constant R is equal to 1.987 cal K^{-1} mol^{-1}.

The values of the parameters of the model are shown in Tables I and II.

For the numerical integration of the differential Eqs. (16)–(21) we have used the Runge-Kutta method. The simu-

TABLE II. Parameters of lateral interactions used in the model. $\varepsilon_{\alpha,X}$ in kcal/mol.

Reaction step, α	$\varepsilon_{\alpha,\mathrm{NO}}$	$\varepsilon_{\alpha,\mathrm{H}}$	$\varepsilon_{\alpha,\mathrm{N}}$	$\varepsilon_{\alpha,\mathrm{O}}$	$\varepsilon_{\alpha,\mathrm{NH}}$	$\varepsilon_{\alpha,\mathrm{NH_3}}$	m_α
3	1.8	0	0	0.8	0	0	4
4	1.5	0	0	0	1.5	0	6
5	1.5	0	0.3	1.8	0	0	6
6	−2	−1	0	−2	−2	−2	6

lations were performed with a tolerance of 10^{-9}.

Autonomous kinetic oscillations

If the partial pressures of the reactant gases are fixed, autonomous oscillations can be observed for certain values of temperature. A sample of these oscillations at $T=434$ K, $p_{\mathrm{NO}}=1.1\times10^{-6}$ mbar, and $p_{\mathrm{H_2}}=7.6\times10^{-6}$ mbar are shown in Fig. 1. There the formation rates of the products H_2O, N_2, and NH_3 [Fig. 1(a)], from greater to lesser oscillation amplitudes, respectively, and the densities of the adsorbed particles NO, NH, H, and NH_3 [Fig. 1(b)], from greater to lesser oscillation amplitudes, respectively, are drawn. The surface coverage of O(ads) and N(ads) are very low during oscillations and they are not shown. The oscillation period is 42 s, similar to that found experimentally. The model also reproduces the experimental results that indicate that the signals of N_2, H_2O, and NH_3 oscillate practically in phase. The mechanism of the oscillations can be explained because when n_{NO} is at a maximum there is a low catalytic activity and the reaction inhibits due to the high coverage of the adsorbate. After a short interval, the NO adlayer reacts and a self-catalytic increase of the vacant number takes place, causing an increase in the reaction rate of the products. Before n_{NO} reaches the minimum value, the densities of the remaining species begin to increase quickly. Finally n_{NO} begins to increase again, the production rates of N_2 and H_2O decrease and the reaction come back to the state with low catalytic activity, starting a new cycle.

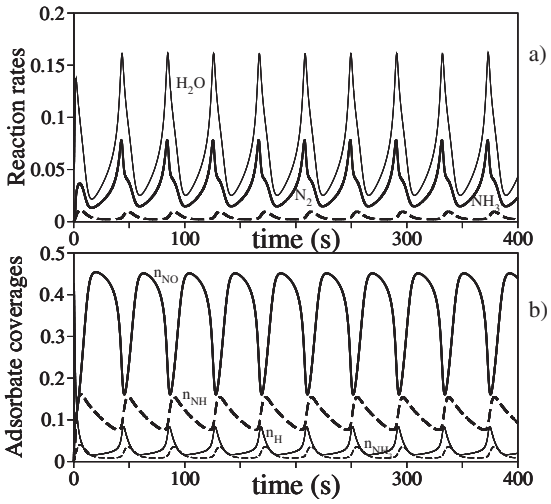

FIG. 1. Time series of the autonomous oscillations of (a) reaction rates of H_2O (thin line), N_2 (thick line) and NH_3 (discontinuous thick line) and (b) surface densities of NO (thick line), NH (discontinuous thick line), H (thin line) and NH_3 (discontinuous thin line). This series corresponds at $T=434$ K, $p_{\mathrm{NO}}=1.1\times10^{-6}$ mbar and $p_{\mathrm{H_2}}=7.6\times10^{-6}$ mbar.

In the experiments, the aperiodic oscillations arise as a result of the period doubling when the partial pressure of H_2 decreases. The transition to aperiodicity occurs in a range very narrow of the control parameter. Even so, the experiments revealed a succession of three bifurcations with period doubling after the solution P1. Moreover oscillations with period-3 (P3) and period-5 (P5) are found in the parametric region where the transition to aperiodic behavior was observed.

The MN model shows excellent agreement with the experiments. They got a bifurcation diagram that revealed the Feigenbaum route to chaos and an approximate structure of the periodic and chaotic windows. The bifurcation diagram was drawn fixing temperature and pressure of NO and decreasing the pressure of H_2 from a high value corresponding to oscillations P1 with large amplitudes. A transition from the state P1 to chaos through successive period doubling is observed when $p_{\mathrm{H_2}}$ decreases. Subsequent decreases of $p_{\mathrm{H_2}}$ lead

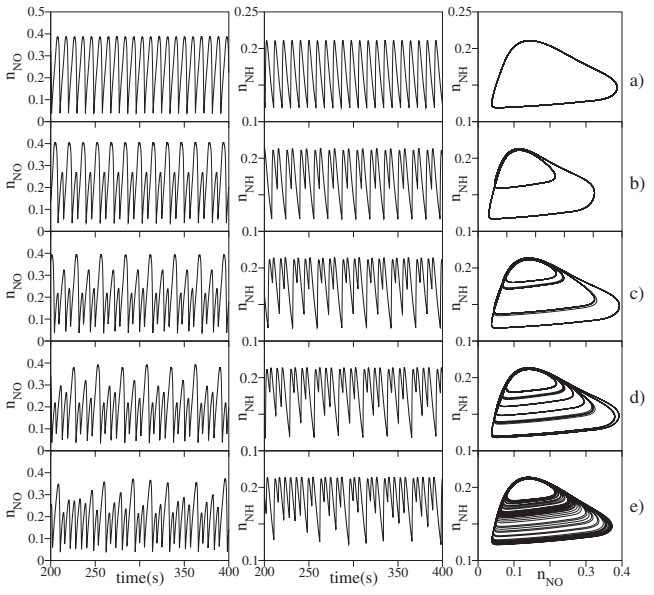

FIG. 2. Route to chaos through period doubling obtained in the autonomous system at $T=457$ K, $p_{\mathrm{NO}}=5\times10^{-6}$ mbar as a function of $p=\frac{p_{\mathrm{H_2}}}{p_{\mathrm{NO}}}$. (a) Period-1, $p=2.52$; (b) period-2, $p=2.50$; (c) period-4, $p=2.46$; (d) period-8, $p=2.4585$ and (e) chaos, $p=2.45$. The left and central columns show the NO and NH coverages, respectively. The right column displays the projections of the different states considered on the $n_{\mathrm{NO}}-n_{\mathrm{NH}}$ plane.

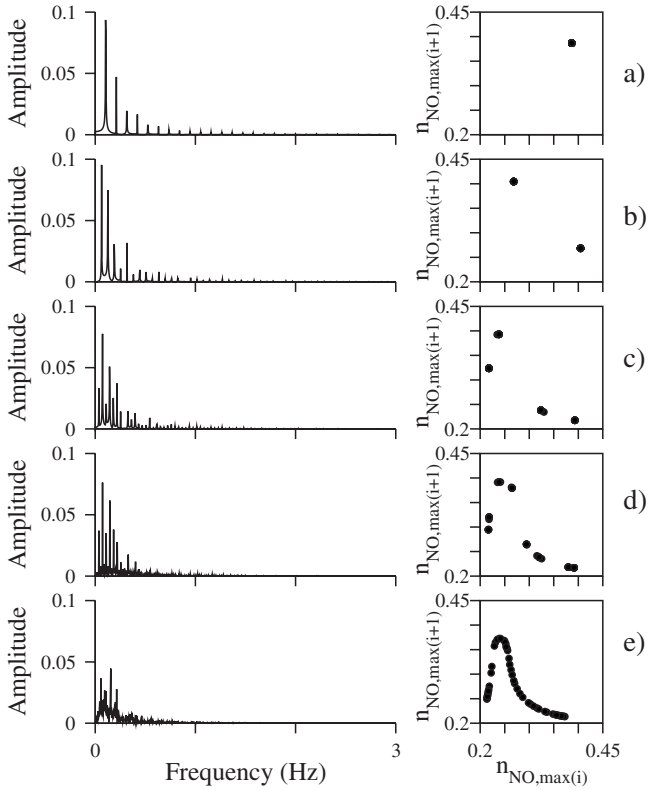

FIG. 3. Fourier spectra and next-maximum maps for the states drawn in Fig. 2. One can observe that the discrete Fourier spectrum becomes a continuous one when the chaotic state is reached. This state is represented by an open line in the next-maximum map.

to a periodic oscillatory state with small amplitude.

Figure 2 shows five representative time series obtained decreasing p_{H_2} and displays the period doubling route to chaos. The calculations were performed fixing temperature $T=457$ K and the partial pressure $p_{NO}=5\times10^{-6}$ mbar. So, the control parameter is the ratio between the pressures of the reactants, $p=\frac{p_{H_2}}{p_{NO}}$. The responses are oscillations (a) P1 ($p=2.52$), (b) P2 ($p=2.50$), (c) P4 ($p=2.46$), (d) P8 ($p=2.4585$), and (e) chaos ($p=2.45$). The two first columns show the time evolution of n_{NO} and n_{NH} and the projection of the state on the n_{NO}-n_{NH} plane is drawn in the third column. The periodic attractors form closed curves and n loops correspond to the oscillatory state with period-n (Pn). The aperiodic oscillations show a great number of loops without no loop passes on the previous one.

Figure 3 shows the Fourier transform and the next-maximum map for the states displayed in Fig. 2. As can be seen, the Fourier spectrum is discrete when oscillations are periodic and it is continuous when oscillations are chaotic. On the other hand, the next-maximum map shows 1, 2, 4, or 8 points depending on the periodic oscillations are P1, P2, P4, or P8, respectively, and an open line, which is characteristic of a chaotic state. There is no doubt about the chaotic character of this last time series. We have calculated, moreover, the maximum Lyapunov exponent and it results 0.034 69, with positive sign, so confirming the chaotic nature of this state.

TABLE III. Ranges of p where the different oscillatory regions of the model are found.

Oscillatory period	$p=\frac{p_{H_2}}{p_{NO}}$	$p=\frac{p_{H_2}}{p_{NO}}$ (Ref. [23])
Period-1	2.512–10.58	2.565–10.27
Period-2	2.462–2.511	2.516–2.564
Period-4	2.4588–2.461	2.5119–2.515
Period-8	2.4585–2.4587	2.5111–2.5118
Chaos	2.4447–2.4584	2.5011–2.511

In Table III the ranges of $p=\frac{p_{H_2}}{p_{NO}}$ where different kinds of oscillations of the model are found are displayed. Our results are similar to those of Caballero and Vicente [23]. They extended the MN model to include defects on the catalytic surface and to consider nonuniformity of the surface in one and two dimensions. As well, they performed Monte Carlo simulations to show the time evolution of the surface densities and to complement the mean field calculations of MN.

Experimentally it has been observed that the reaction of reduction of nitric oxide with hydrogen over Pt(100) shows a great sensitivity to reactant partial pressures, as well as temperature and, as it has been said before, oscillations P3 and P5 were discovered [4]. For conditions slightly different to those taken into account in experiments, the bifurcation dia-

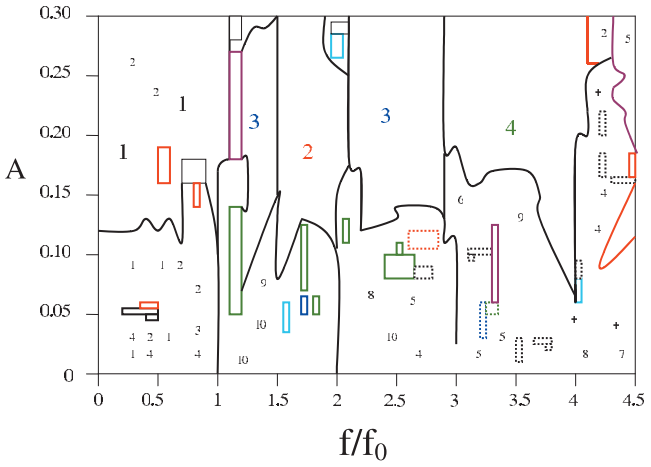

FIG. 4. (Color) Kinetic phase diagram obtained through periodic perturbation of the autonomous model as a function of the normalized amplitude (A) and frequency (f) of the perturbation, the natural frequency being $f_0=0.103\,76$ Hz. The integer k indicates the ratio between the input frequency and the output one in the different regions with periodic oscillations. For high values of A one can observe regions where $k=1$, 2, 3, 4, and 5, denoted by greatest size integers, except narrow chaotic regions (black thin rectangles) embedded among these periodic oscillatory states. In contrast, underneath these periodic regions the behavior is basically aperiodic. One can observe isolated periodic states, denoted by smallest size integers and the symbol $+(k>10)$, and small periodic regions: red, blue, green, prune, and sky blue rectangles indicate $k=2$, 3, 4, 5, and 6, respectively. Red, blue and green broken rectangles indicate periodic areas with $k=7$, 8, and 10, respectively, and black broken rectangles are periodic regions with $k>10$. The black thick rectangles for $A=0.04$ and $A=0.05$ indicate regions with $k=1$.

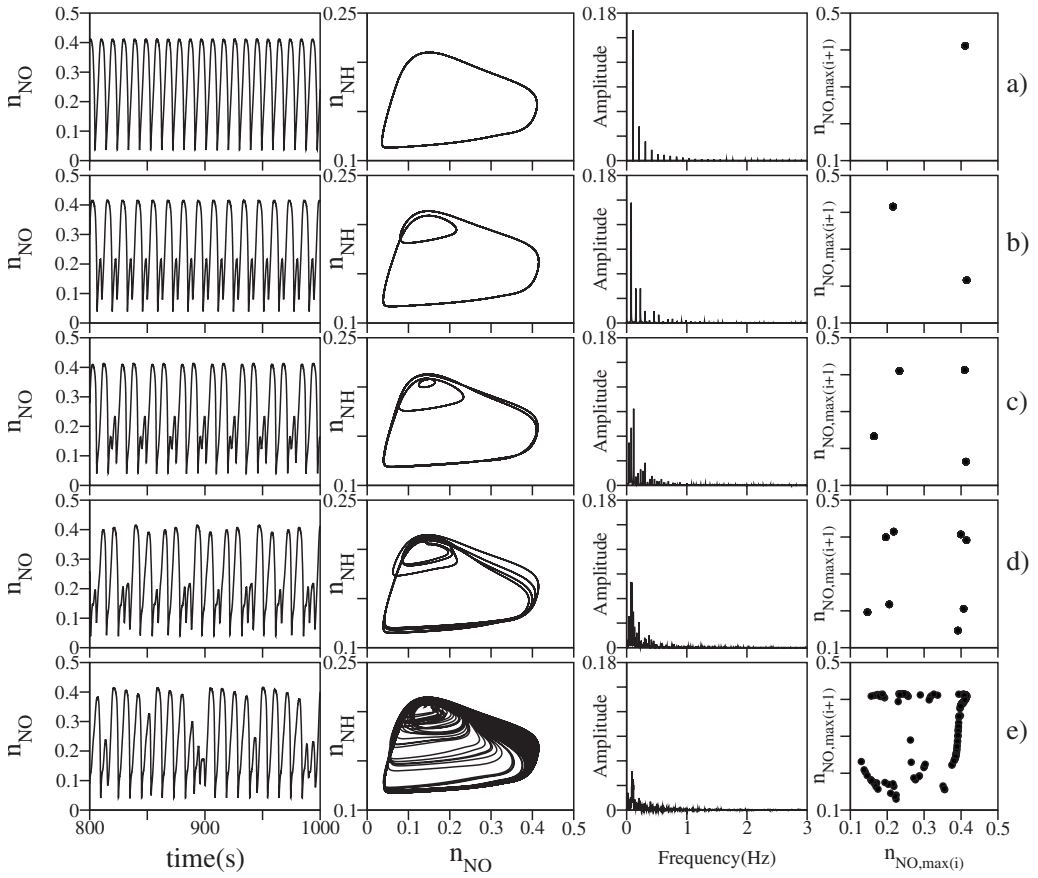

FIG. 5. Route to chaos through period doubling obtained in the perturbed system at $T=457$ K, $p_{NO}=5\times10^{-6}$ mbar, $p=\frac{p_{H_2}}{p_{NO}}=2.52$, $A=0.12$ and (a) period-1 ($f=2f_0$); (b) period-2 ($f=2.2f_0$); (c) period-4 ($f=2.6f_0$); (d) period-8 ($f=3.6f_0$) and (e) chaos ($f=3.8f_0$). The different columns show the time evolution of the NO surface coverage, the projection on the $n_{NO}-n_{NH}$ plane, the Fourier transform and the next-maximum map.

gram of the MN model, at $T=457$ K, which is the temperature considered as reference to analyze the route to chaos in that study, shows states P5 but no P3. The solution P3 is obtained when temperature decreases slightly ($T=456$ K).

III. PERTURBED MODEL

To test the stability of the periodic oscillatory behavior found in the MN model, we have applied a perturbation in the partial pressure of the H_2 gas, using a sinusoidal function with a single frequency

$$p^*_{H_2} = p_{H_2}[1 + A\ \sin(2\pi ft)], \tag{22}$$

where A and f are the normalized amplitude and the frequency of the perturbation, respectively. A systematic variation in A and f will allow us to build the kinetic phase diagram of the perturbed model that will show the different dynamic states of the system and its possible bifurcation points. The values of the other parameters of the perturbed model are the same as in the previous section. Obviously, the perturbation in the reaction rate R_2, which now is written as $R_2=p_{H_2}[1+A\ \sin(2\pi ft)]S_{H_2}k_2n_V^2$, causes as well perturbations in the time change of the surface densities.

In a first step, we choose a state of the autonomous system which exhibits oscillations P1 like that shown in Fig. 2(a), that is to say, at $T=457$ K, $p_{NO}=5\times10^{-6}$ mbar and $p_{H_2}=1.26\times10^{-5}$ mbar ($p=\frac{p_{H_2}}{p_{NO}}=2.52$). This state oscillates with a natural frequency $f_0=0.103\ 76$ Hz (period equal to 9.6 s).

In order to simplify the display of our results, we have chosen n_{NO} as the only output variable because it has the greatest surface density. Each time series corresponds to a pair of values of A and f. In most cases the final regimes have been reached quickly. For these cases we have taken 1600 time steps. We removed the first 600 points to discard with security the transient regime in all cases and with the remaining 1000 points we calculated the time average of n_{NO} and its fluctuation, such that $n_{NO}=\langle n_{NO}\rangle+\theta$. However, the system is close to critical lines until 5000 time steps have been taken to assure the validity of our results. The results are analyzed using the fluctuation of the surface density of NO, θ. Later an analysis of the time series obtained is performed using typical tools of the nonlinear dynamics as the Fourier transform, the Poincaré map or the next-maximum map. Sometimes we have calculated as well the maximum Lyapunov exponent for some of the chaotic states observed.

The kinetic phase diagram of the perturbed model (Fig. 4) is complex and shows a great richness of oscillatory behaviors. The diagram has been realized with an accuracy of 0.01 for the amplitude axis and 0.1 for the frequency axis. In

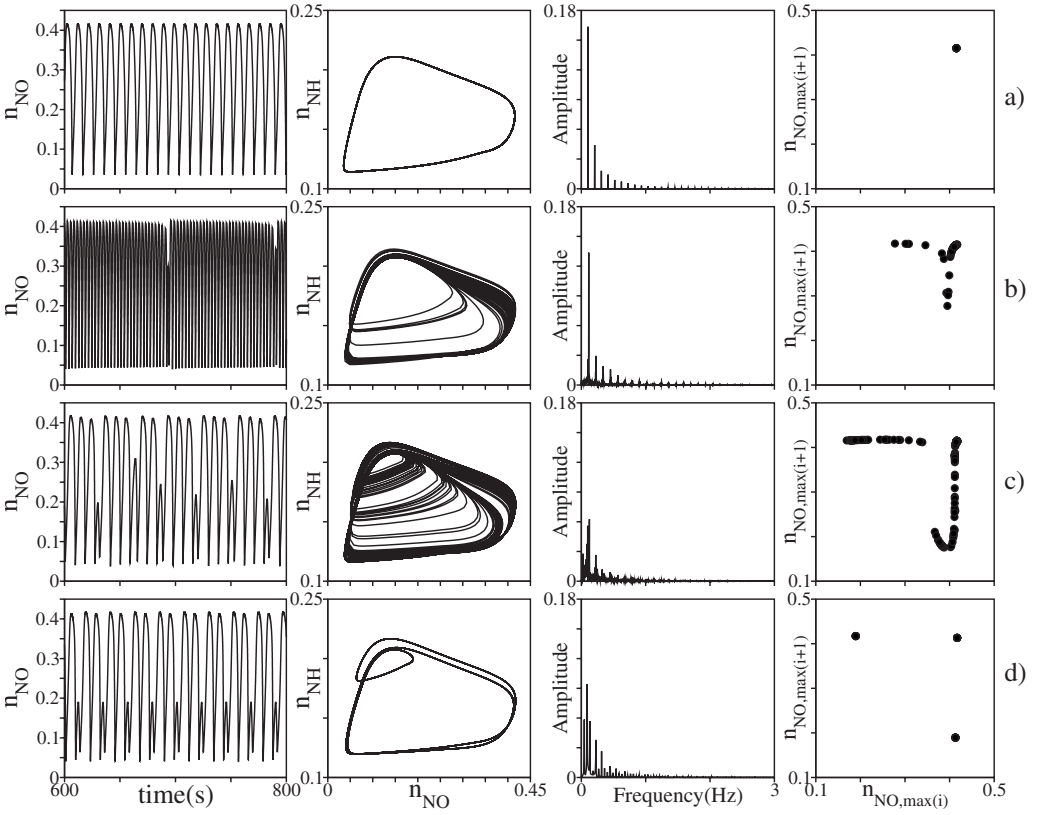

FIG. 6. The different columns show the time evolution of the NO surface coverage, the projection on the $n_{NO}-n_{NH}$ plane, the Fourier spectrum and the next-maximum map obtained in the perturbed system at $T=457$ K, $p_{NO}=5\times10^{-6}$ mbar, $p=\frac{p_{H_2}}{p_{NO}}=2.52$, $A=0.17$ and (a) period-1 ($f=f_0$); (b) intermittency ($f=1.1f_0$); (c) chaos ($f=1.2f_0$) and (d) period-3 ($f=1.3f_0$).

broad outline it observed that if the perturbation amplitude is high ($A\geq0.15$), the response of the system is practically periodic up to values of the frequency of the perturbation $f\leq4f_0$, except the existence of some chaotic states embedded among these periodic states. For $f>4f_0$, aperiodic regions are observed for high amplitudes. When the values of A are low, the periodic regime loses its stability and becomes aperiodic due to the system tends to oscillate with a frequency lesser than its natural frequency. In the transition toward chaotic states we have observed period doubling from an oscillatory state P1 and intermittency processes. These processes take place, in some cases, without displaying the Feigenbaum scenario: the system passed directly from periodic oscillations to chaotic ones. However, we did not observed the appearance of quasiperiodic behavior.

The integer k denotes the ratio between the perturbing and the output frequencies $k=\frac{f}{f_{out}}$, and one can observe regions where $k=1$, 2, 3, and 4 for high values of A and values of frequencies $f\leq4f_0$. These large regions are denoted by the greatest size integers. For frequencies $f>4f_0$, red and prune areas on the right upper corner are observed. These areas correspond to periodic oscillatory regions with $k=2$ (red) and $k=5$ (prune). We have written the integers in bold face. It is also observed a red region ($k=2$, not labeled) for values of amplitudes between $A=0.08$ and $A=0.15$. At high amplitudes (values of A between $A=0.28$ and $A=0.30$) and frequencies ranging from $1.2f_0$ to $1.5f_0$, periodic oscillations with $k=6$ are observed. This region (not denoted) is surrounded by chaotic and periodic areas. Similarly, periodic regions with $k=4$ (not denoted) are obtained for frequencies close to $2f_0$ and values of A between $A=0.25$ and $A=0.30$. This region is also surrounded by periodic area (sky blue rectangle) and chaotic area (black thin rectangle). In general, for high values of $A(A\geq0.15)$, the phase diagram shows periodic oscillatory large regions, except three narrow chaotic regions (black thin rectangles) embedded among these periodic states; two isolated periodic states with $k=2$ (indicated by smallest size number) are also embedded among the periodic region with $k=1$. However, underneath these periodic large regions the behavior is basically aperiodic. One can observe isolated periodic states (labeled by smallest size integers, the symbol + indicating periodic oscillatory states with $k\geq11$), and small periodic regions: red, blue, green, prune, and sky blue rectangles indicate $k=2$, 3, 4, 5, and 6, respectively. Red, blue, and green broken rectangles indicate periodic oscillatory areas with $k=7$, 8, and 10, respectively, and black broken rectangles are periodic oscillatory regions with $k\geq11$. The black thick rectangles for $A=0.04$ and $A=0.05$ indicate regions with $k=1$. The periodic regions that are observed for frequencies $f>4f_0$, have a special characteristic: the oscillation amplitude decreases sharply. These periodic oscillatory states with small amplitude are observed in the autonomous system when p_{H_2} decreases. As well it is observed in the phase diagram that in the regions of periodic oscillations the perturbed system oscillates with a frequency equal or lesser than the perturbing frequency.

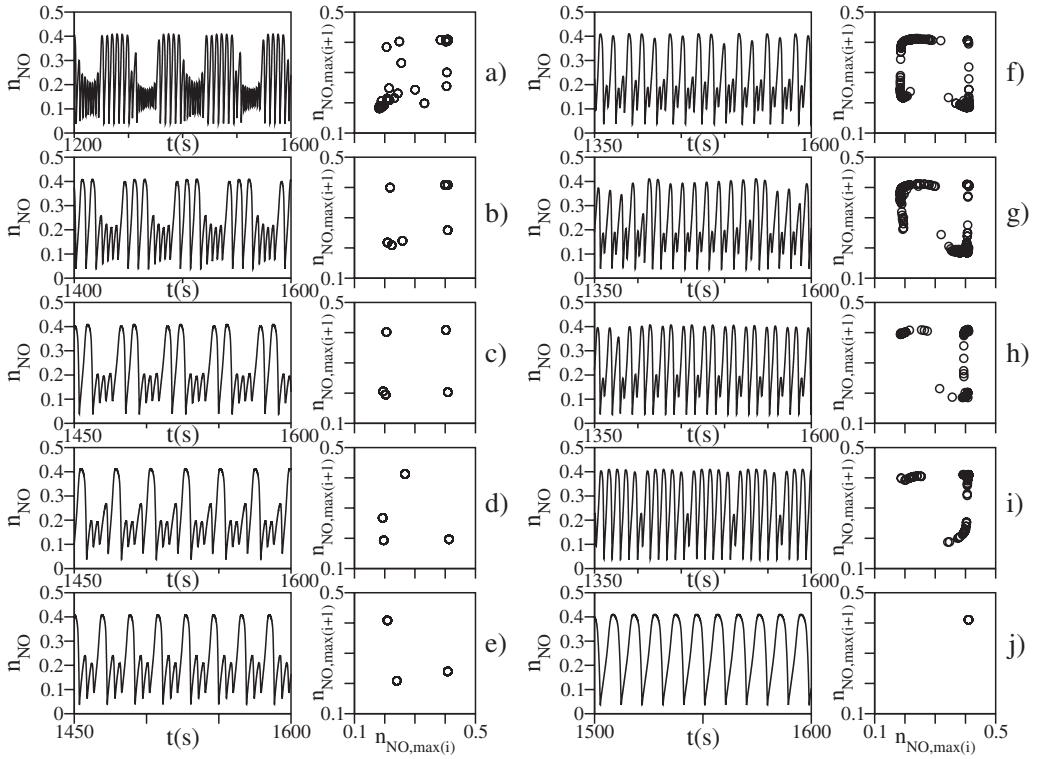

FIG. 7. Time evolution of the NO surface density and next-maximum map of the perturbed system at $T=457$ K, $p_{NO}=5\times10^{-6}$ mbar, $p=\frac{p_{H_2}}{p_{NO}}=2.52$, $A=0.05$ and (a) intermittency ($f=0.1f_0$); (b) period-7 ($f=0.2f_0$); (c) period-5 ($f=0.3f_0$); (d) period-4 ($f=0.4f_0$); (e) period-3 ($f=0.5f_0$); (f) chaos ($f=0.6f_0$); (g) chaos ($f=0.7f_0$); (h) intermittency ($f=0.8f_0$); (i) intermittency ($f=0.9f_0$), and (j) period-1 ($f=f_0$).

The results of the phase diagram show that the response of the natural oscillations P1 with respect to periodic perturbations is diverse. If the perturbing frequency equals to the natural frequency, oscillations P1 are maintained with the imposed frequency. Perturbations with other frequencies may easily change the oscillation P1. We have observed how oscillations P1 are converted to oscillations with different periodicities (P1, P2, P3, …) or to chaotic states which arise as through period doubling bifurcations as through intermittency states. Next these features will be shown.

In Fig. 5 the Feigenbaum route to chaos of the perturbed system is shown at $A=0.12$ and (a) $f=2f_0$ (P1), (b) $f=2.2f_0$ (P2), (c) $f=2.6f_0$ (P4), (d) $f=3.6f_0$ (P8) and (e) $f=3.8f_0$ (chaos). The maximum Lyapunov exponent for this chaotic state is 0.106 63. This figure includes in different columns the time evolution of n_{NO}, the projection on the $n_{NO}-n_{NH}$ plane, the Fourier transform and the next-maximum map for the aforementioned states.

Figure 6 is similar to Fig. 5 and shows, for $A=0.17$, the states (a) P1 ($f=f_0$), (b) intermittency ($f=1.1f_0$), (c) chaos ($f=1.2f_0$) and (d) P3 ($f=1.3f_0$). It appears here the intermittency, which is other of the routes toward chaos. We remark as well the appearance of P3, which is not observed in the autonomous model and which is found experimentally. In fact, MN found this state at temperature $T=456$ K, but they did not observe P3 solution at $T=457$ K.

In Fig. 7 we show through time series and next-maximum maps, fixing $A=0.05$, the evolution of the states of the perturbed system when the perturbing frequency changes. The system passes from an intermittent state for (a) $f=0.1f_0$ to the periodic oscillatory states (b) P7 ($f=0.2f_0$), (c) P5 ($f=0.3f_0$), (d) P4 ($f=0.4f_0$) and (e) P3 ($f=0.5f_0$). Next the system goes to chaotic states, (f) $f=0.6f_0$ and (g) $f=0.7f_0$; to intermittent ones, (h) $f=0.8f_0$ and (i) $f=0.9f_0$; and, finally, to the oscillatory (j) P1 ($f=f_0$).

In Fig. 8 we show again the intermittency phenomenon, which this time occurs near a window of states P2. So, for a fixed value of $f=3.4f_0$, intermittency appears for (a) $A=0.04$, (b) $A=0.05$, (e) $A=0.08$, (f) $A=0.09$ and (g) $A=0.10$, whereas for (c) $A=0.06$ and (d) $A=0.07$ the system exhibits an oscillatory state P2.

Figure 9 displays the drop in the oscillation amplitude when the perturbing frequencies are high. When $A=0.11$, one can see an oscillatory state P1 for (a) $f=4f_0$, that passes to chaotic if (b) $f=4.1f_0$, and the oscillation amplitude decreases when (c) $f=4.2f_0$ (P2) and (d) $f=4.3f_0$ (P1).

The analysis of perturbations of natural oscillations P1 at different frequencies and amplitudes was the goal of our study. To extend this, in a second step, we impose a sinusoidal variation to the perturbation frequency, such that now

$$f=f_0[1+A^*\sin(2\pi f^* t)], \tag{23}$$

f_0 being the natural frequency. The variables f^* and A^* denote, respectively, the frequency and the normalized amplitude modulating the perturbation.

We choose a state of the perturbed system displaying oscillations P1 ($A=0.2$, $f=f_0=0.10376$ Hz) and analyze the response of this state when the perturbing frequency f is modulated according to Eq. (23). We have performed simu-

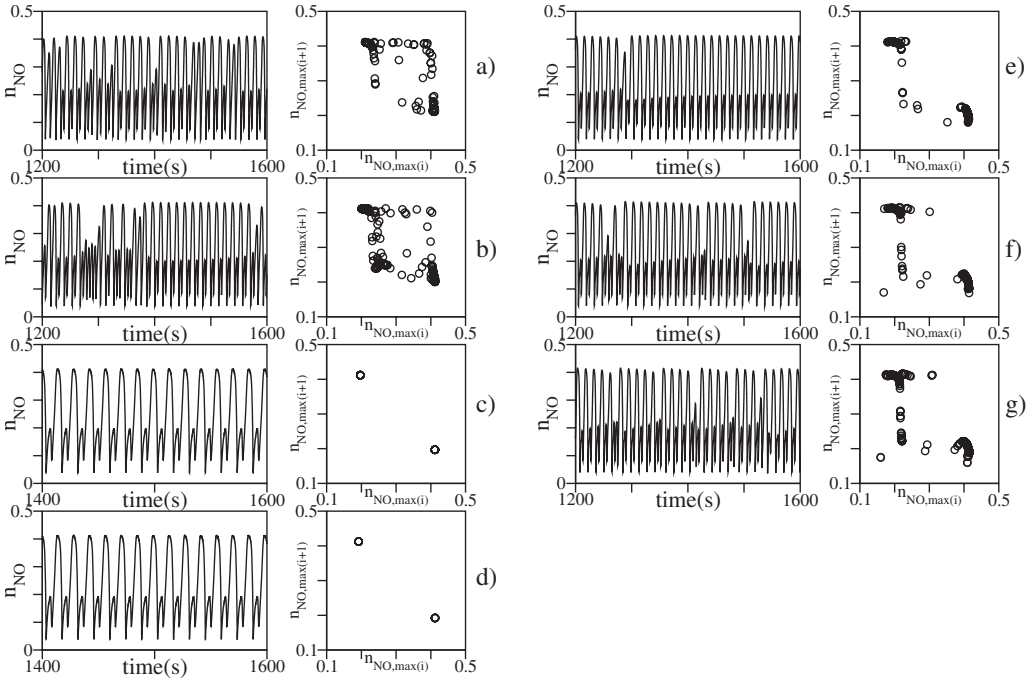

FIG. 8. Intermittency near the window of period-2. The time evolution of the NO surface density and the next-maximum map of the perturbed system are shown at $T=457$ K, $p_{NO}=5\times10^{-6}$ mbar, $p=\frac{p_{H_2}}{p_{NO}}=2.52$, $f=3.4f_0$ and (a) intermittency ($A=0.04$); (b) intermittency ($A=0.05$); (c) period-2 ($A=0.06$); (d) period-2 ($A=0.07$); (e) intermittency ($A=0.08$); (f) intermittency ($A=0.09$) and (g) intermittency ($A=0.10$).

lations for $f_1^*=0.01f$, $f_2^*=0.05f$, and $f_3^*=0.1f$. For each fixed value of f^* the modulating amplitude A^* is varied in 1%, 2%, 3%, 4%, 5%, 10%, 15%, and 20% of the normalized amplitude of the perturbation A. The results obtained are similar in all cases. The states P1 lose their regularity as A^* increases up to finally the periodic oscillation changes to an aperiodic behavior. The appearance of the aperiodic behavior is sooner as f^* is greater. So, periodicity is lost for $A^*=0.1A$ with $f_1^*=0.01f$; for $A^*=0.02A$ with $f_2^*=0.05f$ and for $A^*=0.01A$ when $f_3^*=0.1f$.

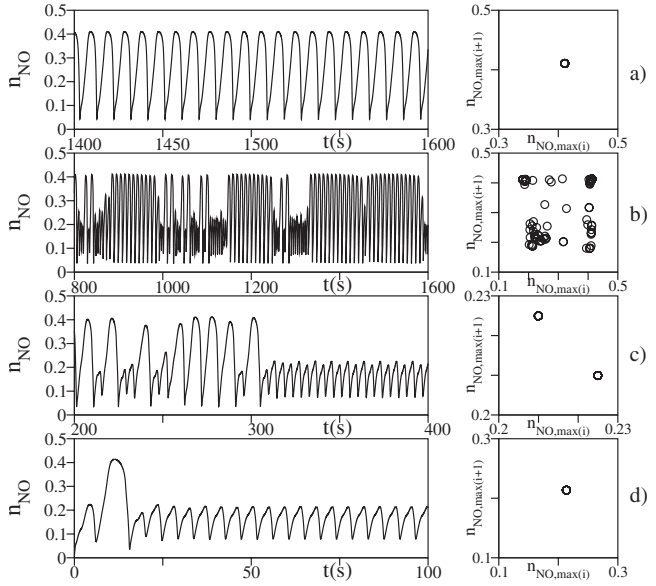

FIG. 9. Drop in the oscillation amplitude when the perturbing frequency is high. The time evolution of the NO surface density and the next-maximum map of the perturbed system are shown at $T=457$ K, $p_{NO}=5\times10^{-6}$ mbar, $p=\frac{p_{H_2}}{p_{NO}}=2.52$, $A=0.11$ and (a) period-1 ($f=4f_0$); (b) chaos ($f=4.1f_0$); (c) period-2 ($f=4.2f_0$) and (d) period-1 ($f=4.3f_0$).

For $A=0.2$, $f=0.10376$ Hz, and $f^*=0.1f$, one can observe in Fig. 10 how the initial behavior (a) P1 ($A^*=0$) disappears as soon as A^* increases. For (b) $A^*=0.01A$, the state P1 begins to modulate by the top side. For (c) $A^*=0.02A$ the chaotic state have established already, remaining for the other perturbing amplitudes (d) $A^*=0.03A$, (e) $A^*=0.04A$, (f) $A^*=0.05A$, and (g) $A^*=0.10A$. Therefore, the periodic structure increases irregularity when the modulating amplitude A^* increases up to, finally, the periodic oscillation is lost.

It is suitable to observe [Table IV, which corresponds to the cases shown in Figs. 5 and 8] that, in general, in the case of periodic forcing, even though the average value of the partial pressure of the H_2 is equal to the constant value of the autonomous case, the average values of the production of H_2O, N_2, and NH_3 are modified, being the values greater or lesser than those in the case nonperturbed. When the state is periodic (Pn) or follows the Feigenbaum route to chaos there is a decrease or a small increase of the production, whereas an increase is produced if there are intermittencies. The greatest increase in percentage (%) takes place for NH_3 production, reaching, for the cases analyzed, approximately up to 10%.

IV. CONCLUSIONS

Summarizing, we have demonstrated, starting from the MN model, which simulates the experimentally observed os-

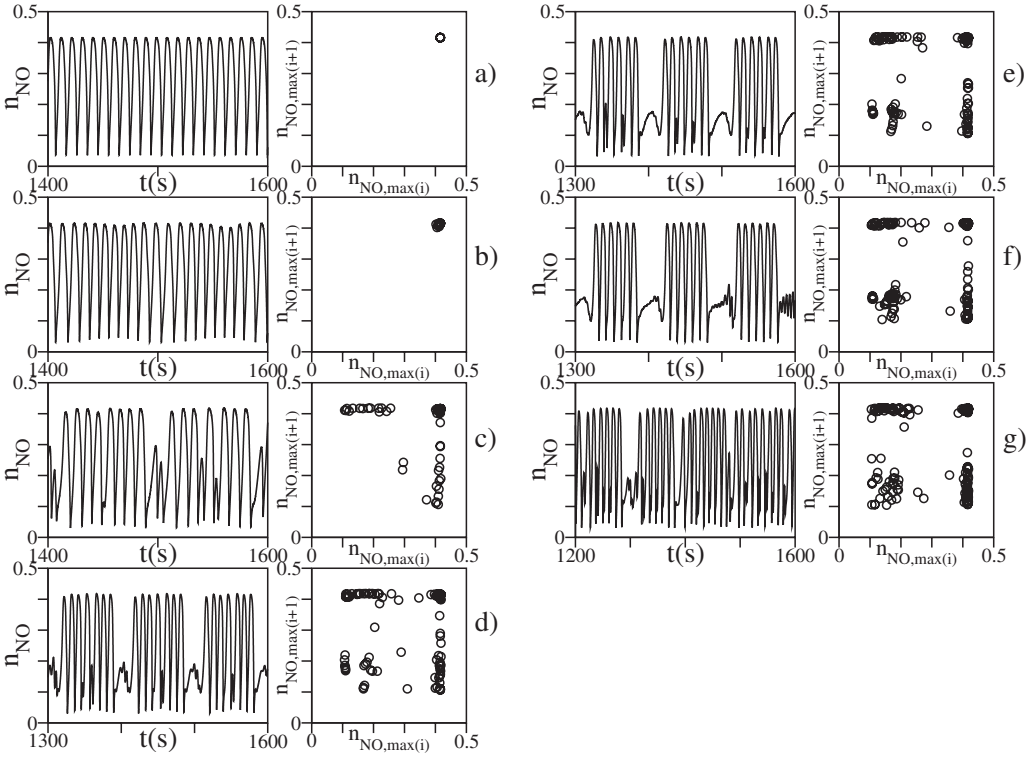

FIG. 10. Time series and next-maximum map that express the response of the oscillations of period-1 observed in the perturbed system at $T=457$ K, $p_{NO}=5\times10^{-6}$ mbar, $p=\frac{p_{H_2}}{p_{NO}}=2.52$, $A=0.2$, and $f=0.10376$ Hz with a perturbing frequency $f^*=0.1f$ and perturbing amplitudes A^* equal to (a) 0, (b) $0.01A$, (c) $0.02A$, (d) $0.03A$, (e) $0.04A$, (f) $0.05A$ and (g) $0.10A$.

cillatory behavior in the heterogeneous catalytic reaction $NO+H_2$ on Pt(100) without to take into account the surface reconstruction [11], that the periodic perturbations on period-1 natural oscillations may easily change these oscillations. Period-1 oscillations are stable with respect to perturbations with a frequency equal to the natural frequency. However, perturbations with other frequencies may shift the type of oscillation. For instance, period-1 oscillations are converted to period-2, period-4, period-8, and chaos (Fig. 5) when the frequencies increase, showing a transition to chaos through period doubling similar to that which is caused by decreasing the partial pressure of the H_2 gas within the autonomous model. It is also observed how period-1 oscillations change to oscillations with period-7, period-5, period-4, and period-3 (Fig. 7) or period-1 oscillations are converted to period-2 oscillations through chaotic states with intermittencies (Fig. 8). Oscillations with different periodicities and chaotic behavior are observed in the perturbed model; still, we have not observed the appearance of quasiperiodic behavior. On the other hand, the results obtained when the pertur-

TABLE IV. Variations in percentage (%) of the average yield of the reaction products in the perturbed model in relation to the nonperturbed model, at $T=457$ K, $p_{NO}=5\times10^{-6}$ mbar, and $p=\frac{p_{H_2}}{p_{NO}}=2.52$.

Amplitude	Frequency	State	H_2O	N_2	NH_3
0.12	$2f_0$	Period-1	−10.9	−12.0	−7.2
0.12	$2.2f_0$	Period-2	−4.0	−5.1	+3.9
0.12	$2.6f_0$	Period-4	−1.8	−2.6	+6.3
0.12	$3.6f_0$	Period-8	+2.0	+1.5	+7.1
0.12	$3.8f_0$	Chaos via Feigenbaum route	−0.6	−1.0	+3.8
0.04	$3.4f_0$	Intermittency	+2.7	+2.4	+7.7
0.05	$3.4f_0$	Intermittency	+2.0	+1.4	+8.6
0.06	$3.4f_0$	Period-2	+0.2	−0.5	+8.5
0.07	$3.4f_0$	Period-2	+0.1	−0.7	+8.5
0.08	$3.4f_0$	Intermittency	+1.5	+0.8	+8.6
0.09	$3.4f_0$	Intermittency	+3.2	+2.7	+9.4
0.10	$3.4f_0$	Intermittency	+3.9	+3.4	+9.7

bation frequency is modulated show that the period-1 oscillations of the perturbed system becomes irregular for low values of the modulating amplitude A^* and frequency f^* of the perturbation.

It is appropriate to indicate that the results of the perturbed model are analogs to others which are obtained when other oscillating chemical reactions are periodically perturbed. However, periodic perturbation of the kinetics of a reaction is an alternative in studies of heterogeneous catalytic reactions, above all with regard to possible limitations as experimental as theoretical. From experimental and models results this reaction reveals a great sensitivity to reactant pressures and temperature. To this effect the period-3 oscillations, that do not appear in the MN autonomous model at $T=457$ K, but they do at slightly lower temperature, are obtained in the perturbed model at $T=457$ K. Moreover, in the perturbed model appears chaos through intermittency. Other effect observed when periodic perturbations are applied on p_{H_2} is that the average yield of the products H_2O, N_2, and NH_3 varies, although the average value of p_{H_2} is equal to the constant p_{H_2} in the nonperturbed model. In the cases considered here, the average yield of products decreases or slightly increases when the oscillations are periodic or they follow the Feigenbaum route to chaos, whereas the average yield of products always increases if there are intermittencies, the increase percentage being more significant for NH_3 (nearly 10%).

ACKNOWLEDGMENTS

This work is partially funded by the Project No. P06-TIC-02025 of the Junta de Andalucía and Project No. FIS2008-04120 of the Spanish Government.

[1] M. W. Lesley and L. D. Schmidt, Surf. Sci. **155**, 215 (1985).
[2] J. Siera, P. Cobden, K. Tanaka, and B. E. Nieuwenhuys, Catal. Lett. **10**, 335 (1991).
[3] H. H. Madden and R. Imbihl, Appl. Surf. Sci. **48/49**, 130 (1991).
[4] P. D. Cobden, J. Siera, and B. E. Nieuwenhuys, J. Vac. Sci. Technol. A **10**, 2487 (1992).
[5] M. Slinko, T. Fink, T. Löher, H. H. Madden, S. J. Lombardo, R. Imbihl, and G. Ertl, Surf. Sci. **264**, 157 (1992).
[6] S. J. Lombardo, M. Slinko, T. Fink, T. Löher, H. H. Madden, F. Esch, R. Imbihl, and G. Ertl, Surf. Sci. **269/270**, 481 (1992).
[7] D. Y. Zemlyanov, M. Y. Smirnov, V. V. Gorodetskii, and J. H. Block, Surf. Sci. **329**, 61 (1995).
[8] R. Imbihl and G. Ertl, Chem. Rev. **95**, 697 (1995).
[9] S. J. Lombardo, T. Fink, and R. Imbihl, J. Chem. Phys. **98**, 5526 (1993).
[10] M. Gruyters, A. T. Pasteur, and D. A. King, J. Chem. Soc., Faraday Trans. **92**, 2941 (1996).
[11] A. G. Makeev and B. E. Nieuwenhuys, J. Chem. Phys. **108**, 3740 (1998).
[12] T. Fink, J.-P. Dath, R. Imbihl, and G. Ertl, J. Chem. Phys. **95**, 2109 (1991).
[13] A. G. Makeev and B. E. Nieuwenhuys, Surf. Sci. **418**, 432 (1998).
[14] V. P. Zhdanov, Surf. Sci. Rep. **55**, 1 (2004).
[15] V. P. Zhdanov, Phys. Rev. E **68**, 056212 (2003).
[16] M. J. Feigenbaum, J. Stat. Phys. **19**, 25 (1978).
[17] Y. Pomeau and P. Manneville, *Intrinsic Stochasticity in Plasmas*, 329 (Editions de Physique, Orsay, France, 1979).
[18] D. Ruelle and F. Takens, Commun. Math. Phys. **20**, 167 (1971).
[19] S. Newhouse, D. Ruelle, and F. Takens, Commun. Math. Phys. **64**, 35 (1978).
[20] A. Córdoba, M. C. Lemos, and F. Jiménez-Morales, J. Chem. Phys. **124**, 014707 (2006).
[21] A. Córdoba, M. C. Lemos, and F. Jiménez-Morales, Phys. Rev. E **74**, 016208 (2006).
[22] M. C. Lemos and A. Córdoba, Catal. Lett. **121**, 121 (2008).
[23] F. V. Caballero and L. Vicente, Chem. Eng. Sci. **58**, 5087 (2003).